한국전자현미경학회지 제 27 권 제 1 호 1997
Korean J. Electron Microscopy 27(1), 101~109(1997)

High-resolution Transmission Electron Microscopy of Ordered Structure for Lead Magnesium Niobate Solid Solutions

Kyeongsoon Park
Department of Materials Engineering, Chung-ju National University,
Chungju, Chungbuk 380-702, Korea

$Pb(Mg_{1/3}Nb_{2/3})O_3$ 고용체에서 고분해능 투과전자현미경을 이용한 구조 규칙화에 대한 연구

박 경 순
충주산업대학교 재료공학과
(Received January 31, 1997)

요 약

La이 첨가되고 또한 첨가되지 않은 $Pb(Mg_{1/3}Nb_{2/3})O_3$ 고용체에서 Mg과 Nb의 비화학양론적인 구조 규칙화 현상이 고분해능 전자현미경과 컴퓨터 이미지 시뮬레이션에 의해 연구되었다. 고분해능 격자 이미지는 여러 이미지 형성 조건과 대물렌즈 구경에서 얻었다. 컴퓨터 이미지 시뮬레이션은 여러 시편 두께, 초점 거리, 장거리 규칙도에서 실시되었다. 규칙격자 구조를 가지는 영역의 격자 이미지는 장거리 규칙도에 크게 의존되는 것이 발견되었다. 규칙격자 구조를 가지는 영역에 있어서, 실험 격자 이미지와 컴퓨터 시뮬레이션 이미지의 비교로부터, 규칙격자 구조를 가지는 영역의 장거리 규칙도는 0.2~0.7의 값을 가지고 있는 것이 관찰되었다. 또한 규칙격자는 $(NH_4)_3FeF_6$ 결정구조를 가지고 있었다.

Key words : 규칙격자, 고분해능 전자현미경, 컴퓨터 이미지 시뮬레이션, 장거리 규칙도

INTRODUCTION

Lead magnesium niobate and other structurally related cubic perovskites, $Pb(B(I)_xB(II)_{1-x})O_3$, are relaxor ferroelectrics. These materials exhibit a high dielectric constant, a relatively low firing temperature, and a diffuse ferroelectric-paraelectric phase transition (Shrout *et al.*, 1987; Chen *et al.*, 1989). Several workers have shown the influence of local chemical fluctuations on the diffuse phase transition by means of order-disorder experiments in perovskite $Pb(Sc_{1/2}Ta_{1/2})O_3$ (PST) and $Pb(Sc_{1/2}Ta_{1/2})O_3$ (PSN) (Setter *et al.*, 1980; Stenger *et al.*, 1980). The diffuse phase transition is largely influenced by the degree in which the B-site atoms are ordered on the B-site sublattice.

It has been reported that ordering in $Pb(Sc_{1/2}Ta_{1/2})O_3$ (PMN) arises due to a composi-

tional segregation, resulting in some regions being Mg-enriched (Köbler *et al.*, 1980; Hüser *et al.*, 1983). These ordered regions were subsequently hypothesized to have local Mg:Nb ratio of 1:1 relative to the global ratio of 1:2, suggesting that a charge imbalance associated with nonstoichiometric ordering may underlie this microstructure and the resultant relaxor behavior (Chen *et al.*, 1989; Randall *et al.*, 1990). The ordered structures of PMN and PST have previously been investigated using X-ray diffraction (Bonneau *et al.*, 1988; Lin *et al.*, 1990) and high-resolution transmission electron microscopy (HRTEM) (Krause *et al.*, 1979; Husson *et al.*, 1988; Kang *et al.*, 1990). However, there is no report on quantitative information, i.e., long-range order parameter, on the ordered structure of the relaxor ferroelectrics. The purpose of this study is to elucidate quantitatively the ordered structure of PMN and to investigate the influence of long-range order parameter on the lattice images of the ordered regions by means of high-resolution lattice imaging and computer image simulation.

EXPERIMENTAL

The samples used in this study were undoped and La-doped PMN solid solutions. These samples were prepared by the precalcination method (Swartz *et al.*, 1982). MgO and Nb_2O_5 were prereacted to form columbite, and then milled with the appropriate proportions of PbO and La_2O_3. La was added to enlarge the size of the ordered domains, increasing the available information concerning the atomic arrangement of the ordered structure.

The samples for HRTEM were prepared by mechanical grinding, dimpling, and then ion-milling at liquid nitrogen temperature. The ion-milling was done using 4.5 keV Ar^+ ions and 1 mA current in order to minimize ion-induced damage. Detailed microstructural information on the ordered region was investigated by HRTEM, which provides all the capabilities necessary for both microstructural and chemical analyses. Especially, the high resolving power of HRTEM allows for quantitative information on the ordered structure of PMN at the atomic level. HRTEM examinations were performed using a Jeol 2000 FX-II transmission electron microscope which was operated at an accelerating voltage of 200 keV. The spherical and chromatic aberration coefficients of the microscope are 2.3 and 2.2 mm, respectively, with resolutions of 0.28 nm (point) and 0.14 nm (lattice). The Scherzer focus of the microscope is ~76 nm. The experimental lattice images of the ordered region were obtained under various defocusing conditions and objective apertures. The experimentally obtained lattice images were compared with the simulated lattice images.

Computer image simulations were carried out using the multislice program (Cowley *et al.*, 1957, 1959(a), 1959(b)) for several sample thicknesses, long-range order parameters, S, and defocusing values of the objective lens, Δf. The multislice program was written by O'Keefe and Skarnulis during the period 1970~1980 (Skarnulis, 1975), and were later modified for IBM software. There are two sets of programs, ZOLT PROG and 3DPROG. The ZOLT PROG does not allow the crystal structure to be varied in the electron beam direction and makes the "projection approximation" or zero order Laue zone (ZOLT) approximation in which the true crystal potential is replaced by its two-dimensional projection through one unit cell in the electron beam direction, while the 3DPROG allows the crystal structure to be varied in the

electron beam direction. The 3DPROG should, thus, be used for structures with a large period in the electron beam direction, for structures non-periodic in the beam direction, e.g., for layer structures with stacking disorder in the beam direction, amorphous structure or surface images, or for the investigation of higher order Laue zone (HOLT) effects. The sample thicknesses ranged from 2.2 to 20.5 nm with a step of 1.1 nm, the long-range order parameters ranged from 1.0 to 0.0, and the defocusing values ranged from −46 to −96 nm with a step of 12 nm. The input microscope parameters used in the computation of the images are the operating voltage, V=200 kV, the radius of objective aperture, r_s=3.37 or 6.05 nm^{-1}, the spherical aberration coefficient, C_s=2.3 mm, the semi-angle of illumination, div=1.0 mrad, the half-width of Gaussian spread of vibration, vib=0.0 nm, and the half-width of Gaussian spread of defocus, del=5 nm. The simulated lattice images were obtained with 420 beams.

RESULTS AND DISCUSSION

The (110) selected area diffraction (SAD) pattern from undoped PMN is shown in Fig. 1. In addition to (strong) allowed reflections originating from the cubic perovskite structure, extra (weak) superlattice reflections, marked by arrows, appear at positions $\left(h+\frac{1}{2},\ k+\frac{1}{2},\ l+\frac{1}{2}\right)$ with respect to the fundamental reflections of the primitive perovskite unit cell (ao 0.402 nm). The existence of these superlattice reflections clearly confirms that there are some regions with ordered structure which results from a doubling ($2a_o \times 2a_o \times 2a_o$) of the primitive perovskite unit cell, as previously reported (Köbler *et al.*, 1980; Hüser *et al.*, 1983). The intensity of the superlattice reflections increased with increasing the contents of the dopant La in PMN, indicating an increase in the size of ordered domains and/or the degree of order. For the Mg: Nb ratio of 1:1, the structure factor $F_{1/2(111)}$ of the 1/2(111) superlattice reflection can be expressed as follows: $F_{1/2(111)}=4(f_{Mg}-f_{Nb})$, where f_{Mg} and f_{Nb} are the atomic scattering factors of Mg and Nb, respectively. This structure factor is a function of the difference of atomic scattering factors of Mg and Nb on the B(I)- and B(II)-sublattices, respectively, and also gives rise to the superlattice spots in the SAD pattern shown in Fig. 1.

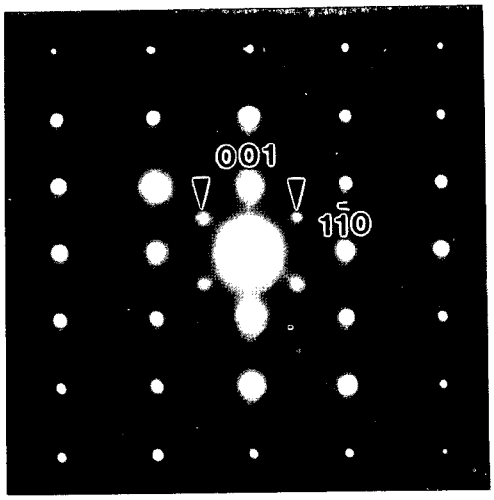

Fig. 1. (110) SAD pattern from undoped PMN. Two superlattice reflectionsare marked by arrows.

In order to investigate the microstructure of the ordered regions for undoped and La-doped PMN at the atomic level, experimental high-resolution lattice images in the [110] projection were obtained under various defocusing values of the objective lens and objective apertures. Thin sample areas (≤20 nm) containing ordered domains with relatively large size (~10-20 nm diameter) were selected for the analyses. This

selection increased the probability of the electron beam to traverse only the ordered regions and not a superposition of ordered and disordered regions. The experimental (110) lattice images from an ordered region under two different defocusing values of the objective lens and objective aperture with radius of 3.37 nm^{-1} for 5% La-doped PMN are shown in Figs. 2(a) and (b). In these figures, a contrast modulation along the (111) directions, and the (001) and (110) lattice fringes with a pseudo-hexagonal pattern are clearly observed. The wavelength of the contrast modulation is ~0.464 nm, which obtained from optical diffractograms taken from the negative of the lattice images. This value approximately equals to twice the calculated (111) interplannar spacing, strongly indicating that the ordered structure arises due to a doubling of the perovskite unit cell.

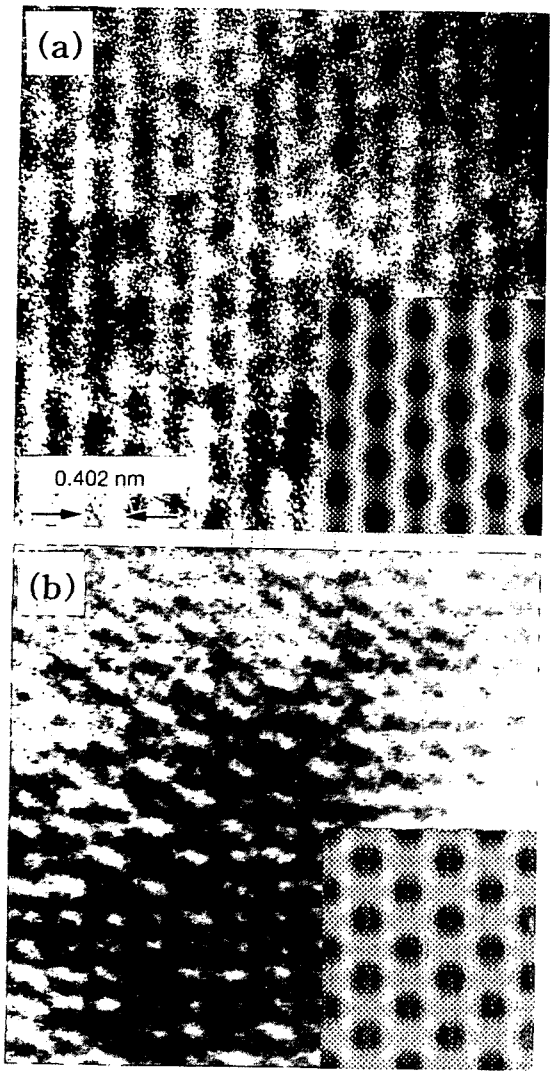

Fig. 2. Experimental (110) lattice images from an ordered region for 5% La-doped PMN under two different defocusing values. The insets show the simulated images for a sample thickness of 12.5 nm, objective aperture with radius of 3.37 nm^{-1}, Mg:Nb ratio of 1:1, long-range order parameter of 0.6, and defocusing values of (a) −64 nm and (b) −76 nm.

Fig. 3(a) and (b) show the (110) lattice images from different ordered region for 5% La-doped PMN under two different defocusing values and objective aperture with radius of 6.05 nm^{-1}. Contrast fluctuations, indicative of the ordered structure, are observed in Fig. 3(a), while essentially no contrast fluctuations are observed in Fig. 3(b), even though both images were obtained from the same ordered region. The lattice image shown in Fig. 3(b) closely resembles that in the disordered regions. It should be therefore noted that the lattice imaging in this alloy system is strongly dependent on the experimental conditions, such as sample thickness and defocusing value.

In order to determine the degree of order of the order region, the experimental lattice images were compared with the simulated lattice images. Simulated images were obtained under five different defocusing values at given sample thicknesses. Computer image simulations were performed using the multislice method, and assuming the ordered $(NH_4)_3FeF_6$ structure (Galasso, 1969) shown in Fig. 4. The Mg and Nb preferred sites on B-site planes can be

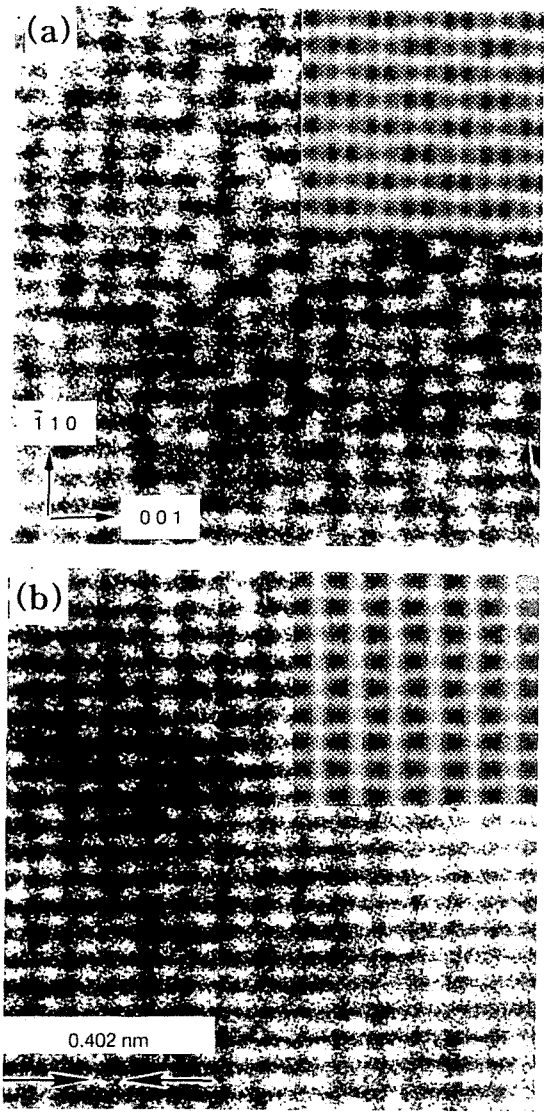

Fig. 3. Experimental (110) lattice images from different ordered region for 5% La-doped PMN under two different defocusing values. The insets show the simulated images for a sample thickness of 12.5 nm, objective aperture with radius of 6.05 nm^{-1}, Mg : Nb ratio of 1 : 1, long-range order parameter of 0.2, and defocusing values of (a) −88 nm and (b) −100 nm.

seen, clearly indicating the 1 : 1 ordering of alternating Mg and Nb layers along the (111) directions. For various occupancies of the Mg and Nb cations on the distinct B-site sublattices, structure factors were calculated and then computer image simulations were performed.

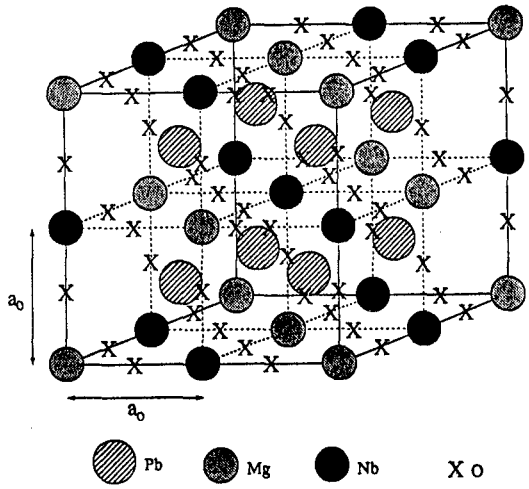

Fig. 4. Proposed model for the atomic configuration of ordered PMN (Galasso, 1969), illustrating the formation of two distinct B-site cation sublattices for Mg and Nb.

For comparison, crystal structure of the ordered perovskite unit cell projected onto the (110) plane is shown in Fig. 5. Open circles, solid circles, hatched circles, open squares denote Mg, Nb, O, and Pb atoms, respectively. This figure shows a preference for Mg or Nb cations on two distinct B-site cation sublattices and alternating Mg and Nb planes along the (111) directions, in which each cation of one B-site sublattice is four-fold coordinated by neighboring cations of the other B-site sublattice.

Fig. 6 shows the pendell sung plots for the intensities of the (001), $(1\bar{1}0)$, $(1\bar{1}1)$, and $\frac{1}{2}$ $(1\bar{1}1)$ beams as a function of sample thickness. These plots indicate that a strong contrast in the $\frac{1}{2}(1\bar{1}1)$ reflection would be achieved for a sample thickness of 16 nm. The total intensity of all beams at this thickness is ~90% of the

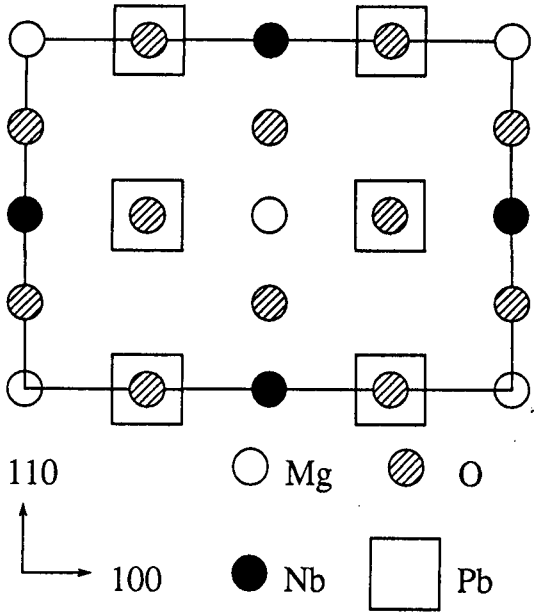

Fig. 5. Crystal structure of the ordered perovskite unit cell projected onto the (110) plane.

incident intensity, implying that only ~10% of the total intensity is lost due to absorption.

Fig. 7 shows the dependence of simulated images on the long-range order parameter and defocusing value at a sample thickness of 16 nm and objective aperture of radius of 3.37 nm^{-1} for local Mg : Nb ratio of 1 : 1. Complete long-range order ($S=1.0$) corresponds to all B(I)- and B(II)-sites being occupied by Mg and Nb, respectively, which can only be achieved for a local Mg : Nb ratio of 1 : 1. The composition of the B-site cations is represented by the atomic fractions C_{Mg} and C_{Nb} of Mg and Nb, respectively, where $C_{Mg}+C_{Nb}=1$. If N is the number of cations on the B-site sublattice, the numbers of Mg and Nb cations are given by $N_{Mg}=C_{Mg}N$ and $N_{Nb}=C_{Nb}N$, respectively. The number of each kind of sites is given by $N_{B(I)}=\nu N$ and $N_{B(II)}=\nu N$, where ν is the fraction of Mg or Nb sites, which for the ordered structure considered in this work is 0.5. The departure from complete order can be described by means of the long-range order parameter S (Smirnov,

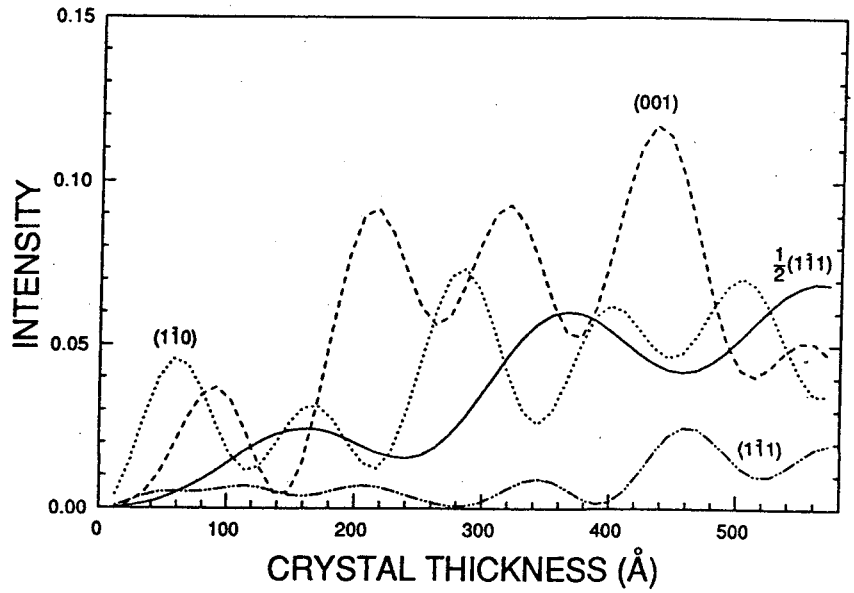

Fig. 6. Pendellösung plots for the intensities of the (001), (1$\bar{1}$0), (1$\bar{1}$1), and $\frac{1}{2}$(1$\bar{1}$1) beams as a function of sample thickness.

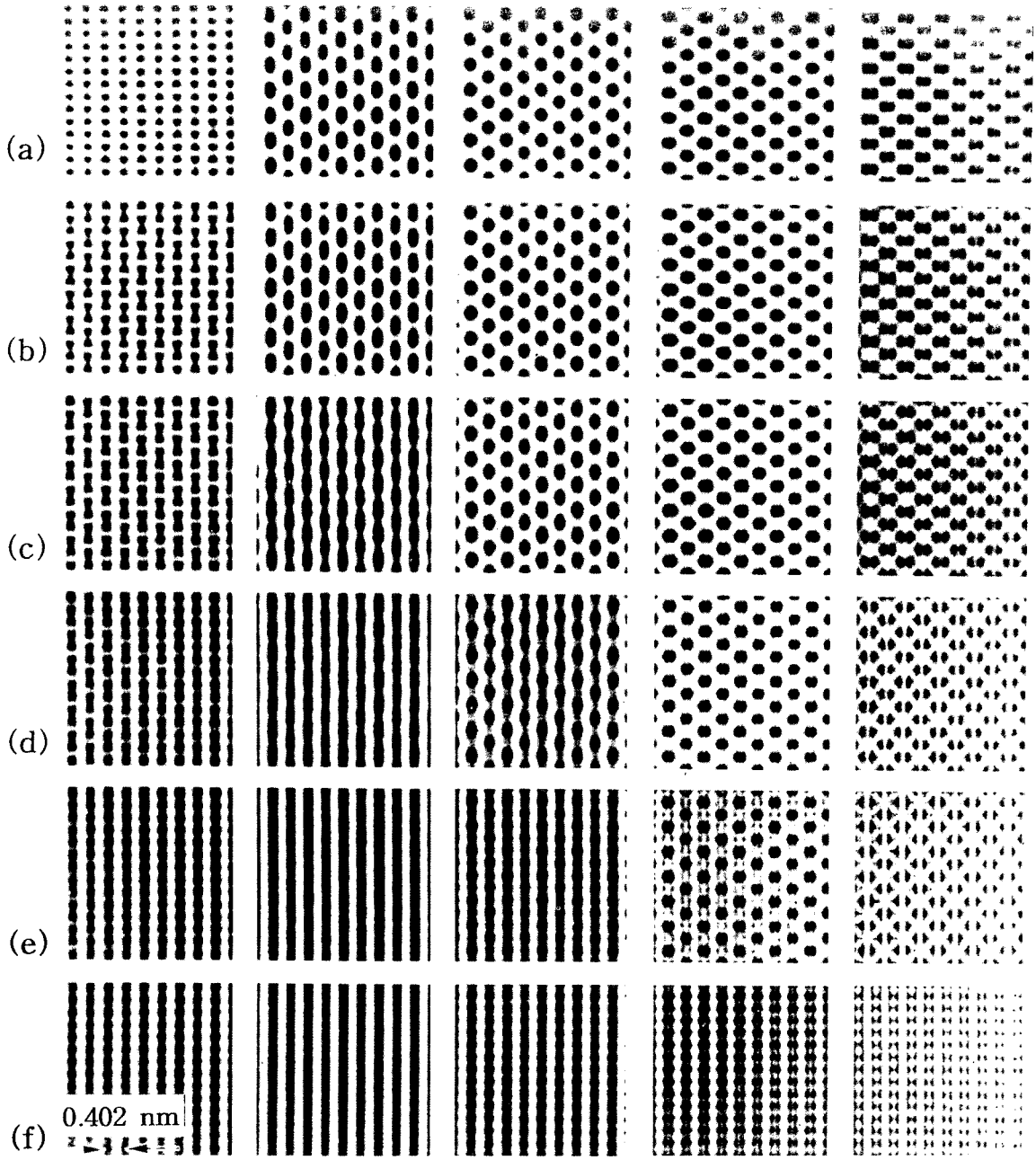

Fig. 7. Simulated (110) lattice images from the local Mg:Nb ratio of 1:1 and sample thickness of 16 nm for long-range order parameter S=(a) 1.0, (b) 0.8, (c) 0.6, (d) 0.4, (e) 0.2, and (f) 0.0. The defocusing values for each column are, from left to right, Δf=−52, −64, −76, −88, and −100 nm.

1966).

$$S=\frac{P_{I(Mg)}-C_{Mg}}{1-\nu}=\frac{P_{II(Mg)}-C_{Nb}}{1-\nu}$$

where $P_{I(Mg)}$ and $P_{II(Mg)}$ are the probabilities of finding a Mg atom at the B(I)- and B(II)-site sublattices, respectively. Thus, the probability

of finding cations at the B(I)- and B(II)-site sublattices can be written as follows.

$$P_{I(Mg)} = C_{Mg} + (1-\nu)S$$
$$P_{I(Nb)} = C_{Nb} - (1-\nu)S$$
$$P_{II(Mg)} = C_{Mg} - \nu S$$
$$P_{II(Nb)} = C_{Nb} + \nu S$$

The maximum order parameter S_{max} in terms of Mg cation composition is defined as (Smirnov, 1966)

$$S_{max} = \frac{C_{Mg}}{\nu}$$

For deviation from 1:1 stoichiometric composition, the order parameter is always less than unity. These simulated images show how the long-range order parameter affects the lattice images. The complete ordered structure ($S=1.0$) has a pseudo-hexagonal pattern. With decreasing the order parameter, the patterns in the calculated images change slowly from a pseudo-hexagonal pattern to a rectangular pattern. The complete disordered structure ($S=0.0$) has a rectangular pattern.

The long-range order parameter of the ordered structure in PMN can be estimated from a comparison of the experimental images and the simulated images by visual observation. The through-focal series of experimental lattice images from the same ordered area were obtained and then compared with the series of simulated images at given values of the order parameters. It is necessary that all the experimental and simulated images in the through-focal series should be matched. The best matches between the experimental and simulated images shown in Figs. 2 and 3 were obtained at $S \approx 0.6$ and $S \approx 0.2$, respectively. The corresponding simulated images are shown as insets to these two figures. The comparisons suggest that the value of the order parameter of ordered regions approximately ranged from 0.2 to 0.7 and also the nonstoichiometric ordering of Mg and Nb cations occurred along the (111) directions. It is not necessary that the local Mg:Nb ratio varies from 1:1 to 1:2 between the ordered and disordered regions. In addition, the comparisons show that the proposed model of $(NH_4)_3FeF_6$ structure for the ordered structure of PMN is valid.

CONCLUSIONS

The nonstoichiometric ordering of Mg and Nb cations was observed in undoped and La-doped lead magnesium niobate solid solutions along the (111) directions. It was found that the simulated lattice images of the ordered regions were strongly dependent on the long-range order parameter. The extensive visual comparison of the experimental and simulated images revealed that the value of the order parameter in the ordered regions approximately ranged from 0.2~0.7 and also the ordered regions had a $(NH_4)_3FeF_6$ structure. Furthermore, the complete ordered structure ($S=1.0$) showed a pseudo-hexagonal pattern. As the order parameter decreased, the patterns in the calculated images changed slowly from a pseudo-hexagonal pattern to a rectangular pattern.

ABSTRACT

The nonstoichiometric ordering of Mg and Nb cations in undoped and La-doped lead magnesium niobate solid solutions has been investigated by means of high-resolution transmission electron microscopy and computer image simulation. High-resolution lattice images were obtained under various microscope imaging conditions and objective apertures. Computer image simulations

were performed for a wide range of sample thickness, defocusing value, and long-range order parameter. The simulated images revealed that the lattice images of the ordered regions were predominantly dependent on the long-range order parameter. From the comparisons of the experimental and simulated images for the ordered regions, the long-range order parameter approximately ranged 0.2 to 0.7. It was also found that the ordered structure has a $(NH_4)_3FeF_6$ structure, which consists of alternating Mg- and Nb-preferred sublattices along the (111) directions.

REFERENCES

Bonneau P, Garnier P, Husson E, Morell A, 1988. Structural study of PMN ceramics by X-ray diffraction between 297 and 1023 K. Mater. Res. Bull. 24, 201-206.

Chen J, Chan HM, Harmer MP, 1989. Ordering structure and dielectric properties of undoped and La/Na-doped $Pb(Mg_{1/3}Nb_{2/3})O_3$. J. Amer. Ceram. Soc. 72, 593-598.

Cowley JM, Moodie AF, 1957. The scattering of electrons by atoms and crystals. I. A new theoretical approach. Acta Crystallogr. 10, 609-619.

Cowley JM, Moodie AF, 1959(a). The scattering of electrons by atoms and crystals. II. The effects of finite source size. Acta Crystallogr. 12, 353-359.

Cowley JM, Moodie AF, 1959(b). The scattering of electrons by atoms and crystals. III. Single-crystal diffraction patterns. Acta Crystallogr. 12, 360-367.

Galasso FS, 1969. Structure, Properties and Preparation of Perovskite-Type Compounds, ed. R. Sinoluchowski and N. Kurti, Pergamon Press, New York, p. 12.

Hüser D, Wenger LE, Van Duyneveldt AJ, Mydosh JA, 1983. Dynamical behavior of the susceptibility around the freezing temperature in (Er, Sr)S. Phys. Rev. B27, 3100-3103.

Husson E, Chubb M, Morell A, 1988. Superstructure in $Pb(Mg_{1/3}Nb_{2/3})O_3$ ceramics revealed by high resolution electron microscopy. Mater. Res. Bull. 23, 357-361.

Kang ZC, Caranoni C, Siny I, Nihoul G, Boulesteix C, 1990. Study of the ordering of Sc and Ta atoms in Pb_2ScTaO_6 by X-ray diffraction and high resolution electron microscopy. J. Solid State Chem. 87, 308-320.

Köbler U, Binder K, 1980. Paramagnetic susceptibility of $Eu_xSr_{1-x}S$: Experiment and comparison with high-temperature series expansion. J. Magn. Magn. Mater. 15-18, 313-314.

Krause HB, Cowley JM, Wheatley J, 1979. Short-range ordering in $Pb(Mg_{1/3}Nb_{2/3})O_3$. Acta Crystallogr. A35, 1015-1017.

Lin LJ, Wu TB, 1990. Ordering behavior of lead magnesium niobate ceramics with a-site substitution. J. Amer. Ceram. Soc. 73, 1253-1256.

Randall CA, Bhalla AS, 1990. Nanostructural-property relations in complex lead perovskites. Jpn. J. Appl. Phys. 29, 327-333.

Smirnov A, 1966. Molecular Kinetic Theory of Metals, Nauka Press, Moscow, p. 185.

Setter N, Cross LE, 1980. The role of B-site cation disorder in diffuse phase transition behavior of perovskite ferroelectrics. J. Appl. Phys. 51, 4356-4360.

Shrout TR, Halliyal A, 1987. Preparation of lead-based ferroelectric relaxors for capacitors. Amer. Ceram. Soc. Bull. 66, 704-711.

Skarnulis AJ, 1975. Ph. D. Dissertation, Arizona State University.

Stenger CGF, Burggraaf A, 1980. Order-disorder reaction in the ferroelectric perovskites $Pb(Sc_{1/2}Nb_{1/2})O_3$ and $Pb(Sc_{1/2}Nb_{1/2})O_3$. Phys. Stat. Solidi (a) 61, 275-285.

Swartz SL, Shrout TR, 1982. Fabrication of perovskite lead magnesium niobate. Mater. Res. Bull. 17, 1245-1250.